Experimental and Numerical Analysis of Cellulosic Insulation Failures of Continuously Transposed Conductors under Short Circuits and Thermal Ageing in Power Transformers

C. Oria[1], I. Carrascal[2], A. Ortiz[1], I. Fernández[1], D. Ferreño[2], R. Afshar[3] and **K. Gamstedt[3]**
[1]Electrical and Energy Department, University of Cantabria
[2]Laboratory of Science and Engineering of Materials, University of Cantabria
Avenida Los Castros, s/n, 39005, Santander, SPAIN
[3]Department of Engineering Sciences, The Ångström Laboratory, Uppsala University
Lägerhyddsvägen 1, 752 37, Uppsala, SWEDEN

ABSTRACT

The integrity of the cellulosic insulation in power transformers is considered one of the most relevant parameters that affects their performance and reliability. Electric faults, such as short circuits, have thermal and mechanical effects that degrade the paper and can eventually produce the end-of-life of the transformer. The evolution of the properties of the paper insulation of a commercial continuously transposed conductor due to thermal ageing was characterised through the degree of polymerisation and tensile testing. Failure initiation and propagation in the paper was analysed macroscopically and microscopically using scanning electron microscope. A finite element numerical mechanical model of the conductor was implemented to reproduce the experiments and to obtain the load level and strain state that produce failure at each ageing state, aiming at developing a failure model for the insulation. This model may contribute to an improvement in manufacturing processes and management of the electrical system.

Index Terms — **power transformers, insulation, short circuits, accelerated ageing, mechanical behaviour, numerical simulation, failure analysis**

1 INTRODUCTION

THE world as we know it today would not be possible without electricity transmission, which is essential for almost every human activity and has been of vital relevance for the progress of industry and society. Power transformers play a crucial role in the electrical system, where the reduction of operating costs, the enhancement of the reliability of transmission, distribution and interconnection, and the improvement of the quality of power supply to the consumers are of vital importance.

In the transformer, the insulation between two components at different potential consists of several oil-impregnated paper sheets placed perpendicularly to the electric field gradient [1]. Many factors affect the correct operation of power transformers and reduce their useful-life, and one of them is the state of that insulation, which is subjected to high temperatures and mechanical stresses, generated by static and dynamic loads, such as the ones produced by short circuits. Moreover, chemical reactions take place in the dielectric oil, contributing to its ageing. As the insulation ages, both its electrical properties (such as resistivity or dielectric breakdown strength) and its mechanical properties (tensile strength or ultimate elongation) gradually deteriorate. Some authors consider that those mechanical and electrical properties are significantly related [2].

This work analyses the response of a commercial continuously transposed conductor (CTC) of a core-type transformer, with disc-type cylindrical windings. The CTC is made of enamelled annealed copper and covered in four layers of dielectric paper, each with a thickness of 80 μm. Several samples of that CTC were impregnated in naphthenic dielectric oil and subjected to accelerated thermal ageing, to reproduce the process that takes place after several years of operation in a power transformer. The cellulosic insulation was removed from some samples and mechanically characterised, and other CTC samples were subjected to bending tests, in an attempt to make a simplified representation of the effects of electromagnetic forces generated by short circuits. After these tests, fracture patterns of the insulation layers were analysed.

A simulation model was developed in ANSYS AIM, introducing the geometrical and constitutive characteristics of the CTC, in order to reproduce the bending test and to obtain the strain field in the conductor under those conditions. As a very similar strain field will appear in the paper insulation in which the copper is wrapped, a failure model could be developed to predict the critical load state that leads to failure.

Manuscript received on 22 July 2019, in final form 1 November 2019, accepted xx Month 20yy. Corresponding author: C. Oria.

This paper contributes to extending some previous analyses (such as [3–7]), to understand the mechanical response and degradation processes which could lead to the end of life of transformers. There are many studies analysing the mechanical behaviour of cellulosic materials, but only a few of them are specific for the insulation of transformers (such as [8–12]). At present, there are no experimental results analysing how the paper responds to the deformation suffered by the conductor in an approximately realistic situation. The development of a suitable failure model for paper insulation, in combination with engineering measurements, could help to accurately predict the end-of-life of power transformers and to improve the manufacturing techniques, to obtain more reliable components.

In this paper, first, the experiments are described (the thermal ageing of the insulation, its mechanical characterisation, the bending tests over the CTC samples and the failure of the insulation). Then, the numerical simulation is detailed, and its results are correlated with the experimental observations.

2 EXPERIMENTAL

2.1 ACCELERATED THERMAL AGEING OF PAPER INSULATION

A very long time would be needed to study the effects of ageing if the temperature is maintained within realistic values in operating transformers, so shorter experiments at elevated temperature are widely used. In this study, 20 test samples with a length of 120 mm, Figure 1a, were extracted from the copper coil, vacuum-dried in an oven at 100°C for 3 hours, up to a final moisture content of 1.99%, measured according to [13].

Figure 1. (a) CTC sample with the principal directions of the paper, MD and CD; (b) test pieces in the vessel filled with dielectric oil.

Five different ageing states were considered in the analysis. Four samples were not aged (*Ageing State 0*). The other samples were introduced into sealed vessels filled with naphthenic dielectric oil (four samples in each vessel), Figure 1b, with a ratio of 10 g paper/400 g oil. The vessels were vacuum-sealed, and an inert atmosphere was created by filling them with nitrogen. Finally, they were introduced into temperature-controlled ovens and aged at 150ºC for 1 week (*Ageing State I*), 4 weeks (*Ageing State II*), 9 weeks (*Ageing State III*) and 28 weeks (*Ageing State IV*). After the ageing process, the samples were washed five times, with hexane, to remove the remaining oil from the paper. The degreased material was then dried by exposing it to the open air, to be later characterised.

2.2 CHARACTERISATION OF PAPER SAMPLES

Two samples from each of the four layers were extracted from one CTC sample of each ageing state (five conductor samples x 4 layers x 2 samples per layer = 40 paper samples), to be subjected to tensile tests. The mechanical properties were determined in the two principal in-plane directions, the machine direction (MD) and the cross direction (CD); in addition, several samples of each layer were used to measure the degree of polymerisation. In the insulation, the internal layers (1 and 2) were made of plain Kraft paper and the external ones (3 and 4) of crepe paper. We were interested in determining whether thermal ageing has a different effect on the layers depending on their position, as layers 1 and 4 are in direct contact, respectively, with the enamelled CTC and with the dielectric oil, while layers 2 and 3 are between the two.

2.2.1 Degree of polymerisation (DP) of paper

The average viscometric degree of polymerisation, $\overline{DPv}$, of new and aged cellulosic materials for insulating use can be determined according to [14]. For very thin papers, the material must be cut into small pieces, separating the cellulose fibres to facilitate dissolution in the solution, which in this case consisted of 22.5 ml of deionised water and 22.5 ml of copper (II) ethylenediamine. The solution was stirred for 48 hours. The results of the DP measurement can be seen in Figure 2.

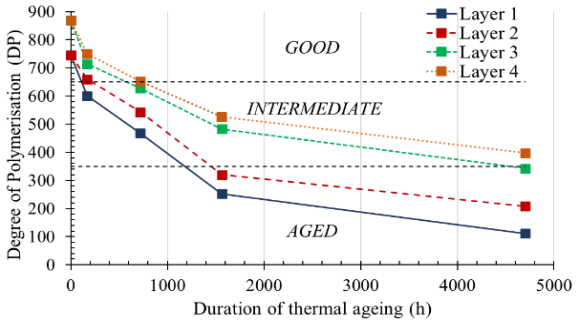

Figure 2. State of the different layers of the insulation according to the classification of [14], as a function of the duration of thermal ageing.

The non-aged material has a value of the DP catalogued as "good" in [14], and crepe paper has a higher initial DP, which is related to its better mechanical properties. The initial reduction in DP after one week of ageing was very similar for both materials (15.4% for the inner layers and 15.9% for the crepe paper). Between Ageing States I and III, the reduction in DP seems to be approximately linear. After four weeks, the ageing of all the layers was intermediate (DP between 350-650) and layer 1 was the most deteriorated. After Ageing State III, the internal layers were in an aged condition (DP < 350) while the external ones remained in an intermediate condition.

At the end of the ageing process, in State IV, the DP had decreased 85% in layer 1, 72.2% in layer 2, 60.6% in layer 3 and 54.4% in layer 4 (with respect to State 0). Being in contact with the CTC increased the deterioration, while no especially harming effect was reported in the most external layer.

2.2.2 Tensile properties of paper

The standard [15] specifies a method for the measurement of tensile strength, elongation to break and tensile stiffness of paper and paperboard samples with length of 180 ± 1 mm and width of 15 ± 0.1 mm, subjected to tensile up to fracture with a constant rate of elongation of 20 mm/min, which is equivalent to a strain rate of: $\dot{\varepsilon} = \frac{\varepsilon}{t} = \frac{\frac{20mm}{180mm}}{60s} \simeq 0.00185\ s^{-1}$. When the product has limited size, [15] allows the use of smaller sample dimensions. Here, samples of 140 mm x 15 mm were used for the characterisation in MD (100 mm between grips of the machine), Figure 3, because it was the only way to obtain two

paper samples from each layer. A rate of elongation of 11.11 mm/min was used to maintain the proposed strain rate.

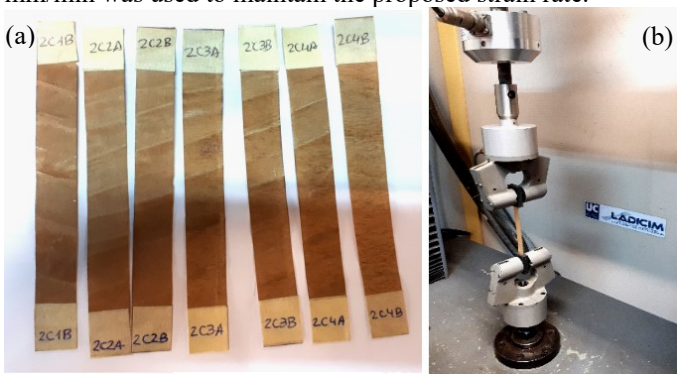

Figure 3. (a) Some paper samples of Ageing State II. (b) Tensile test for the characterisation of the paper samples in MD.

Figure 4 shows the results of tensile tests in MD for the same layer and different ageing states. The mechanical properties of the plain Kraft paper (Figure 4a), which behaves as a purely plastic material, radically differ from the crepe paper (Figure 4b), which has a hyperelastic response, displaying a much greater strain at break (ε_{MD}^{max}). The curves represented here are an average representative response, but the experiments showed in some cases a noticeable scatter for two samples obtained from the same layer and ageing state. For instance, the average coefficient of variation of ε_{MD}^{max} for all the tensile tests in the different ageing states was approximately 8.6% for layer 1, 8.8% for layer 2, 6.4% for layer 3 and 3.7% for layer 4. The degree of heterogeneity of the material was mainly due to its own microstructure and, especially, to local defects (micro cracks or small delaminations) sometimes produced during manufacturing of the insulated CTC.

A temperature of 150ºC was chosen so that the crepe paper insulation (layers 3, 4) reaches a DP ≃ 350 (aged conditions) after a reasonable ageing duration. A lower ageing temperature would have required ageing periods of more than seven months. However, the enamel melted during the heating because its thermal class was not sufficient to withstand 150ºC; as a result, layer 1 and the CTC were glued, so layer 1 was considerably deteriorated. Consequently, the reduction in stiffness of layer 1 was not totally representative of the material response under normal operating conditions and can be regarded as a representation of what would happen if a transformer is accidentally subjected to more extreme conditions than its rated ones. On the other hand, the enamel melting did not affect layers 2, 3 and 4 of the insulation, so their mechanical response and failure modes can be considered fully representative.

The variation in the tensile strength in MD due to ageing can be seen in Figure 5a. The initial reduction of strength was maximum in layer 1, and an unexpected result was obtained in the other layers: the strength seemed to be higher in Ageing State I than when the paper was not aged. The reason could be that the initial impregnation in dielectric oil filling the voids in the paper improves its mechanical resistance in comparison with the paper alone, although this improvement was not appreciated in the ε_{MD}^{max}. After one week of ageing, the strength started decreasing up to the end of the process. Although the initial strength of the plain Kraft was lower than that of the crepe paper, the strength of layers 3 and 4 suffered a higher descent between Ageing States I and IV.

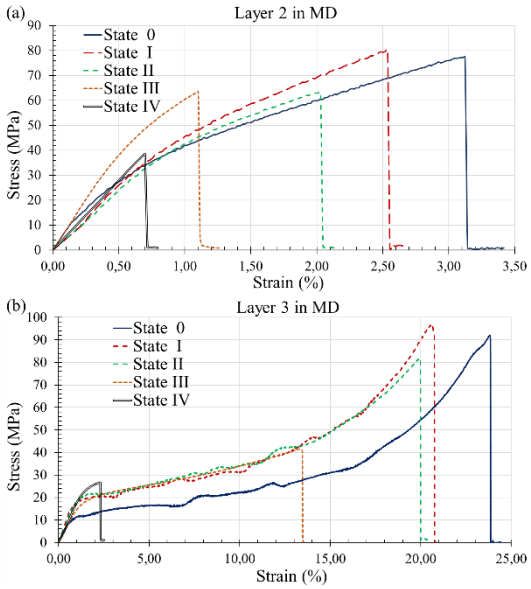

Figure 4. Tensile test in MD for (a) plain Kraft paper, and (b) crepe paper in the different ageing states.

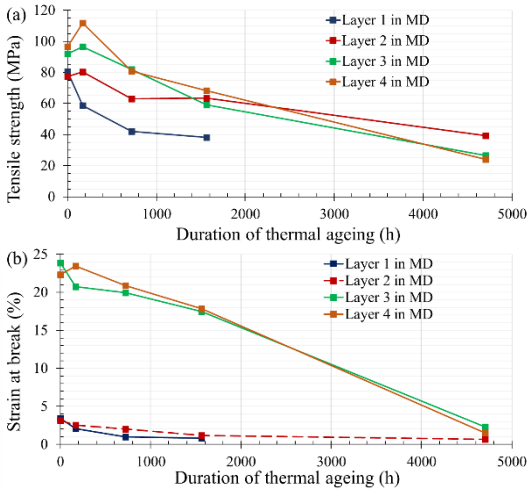

Figure 5. (a) Tensile strength and (b) strain at break in MD as a function of ageing duration.

Regarding the variation in strain in MD, Figure 5b, there was a great difference in the initial ε_{MD}^{max} of plain and crepe papers. For the first one, the decrease in strain was maximum in the first hours of ageing, and less accused up to the end of the process. For the crepe paper, the decrease was more marked after State II. At the end of the thermal ageing duration, both materials were very fragile and had similar values of the strain at break.

The characterisation of the material in CD was a technical challenge, because of the narrowness of the insulation strips. The tested paper samples had an average length of 17 mm and a width of 15 mm and, as those dimensions were remarkably different to those recommended in [15], the elongation rate was reduced proportionally, up to 1.7 mm/min. Figure 6 shows the results of some tensile tests in CD for the same layer and different ageing states. As expected, the tensile strength was lower in CD: for the plain Kraft, the tensile strength in CD was approximately 50% of the value in MD, and only 15% for the crepe paper.

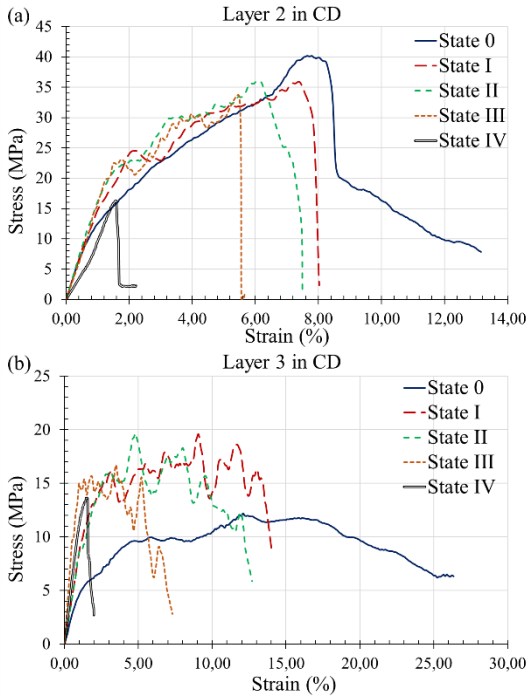

Figure 6. Tensile test in CD for (a) plain Kraft paper, and (b) crepe paper in the different ageing states.

The evolution in the tensile strength in CD can be seen in Figure 7a. The variation in strain in CD, Figure 7b, shows that the ε_{MD}^{max} was higher than ε_{CD}^{max} for the crepe paper, but the opposite happened with the plain Kraft. At the end of the ageing process, the strain at break had similar values for both materials, and both in MD and CD.

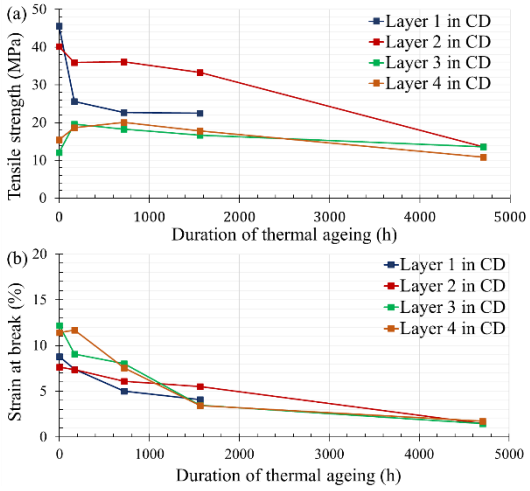

Figure 7. (a) Tensile strength and (b) strain at break in CD as a function of ageing duration.

2.3 BENDING TESTS OF THE INSULATED-CTCs

2.3.1 Short-circuit forces in power transformers

Short circuits produce a transient temperature rise in the windings that does not usually represent a serious problem, but the electromagnetic forces produced can be about 100-400 times the forces under normal operating conditions [1]. The force density vector is the product of the current density vector and the magnetic flux density: $\overline{f(t)} = \overline{J(t)} \times \overline{B(t)}$, and has only two components in the cylindrical coordinate system of a core-type transformer with disc-type windings, Figure 8a: the radial, $f_r(t)$, and the axial one, $f_z(t)$. As the bending stiffness of the CTC is much lower in radial than in axial direction, and also for the sake of simplicity, a radial bending force was considered here.

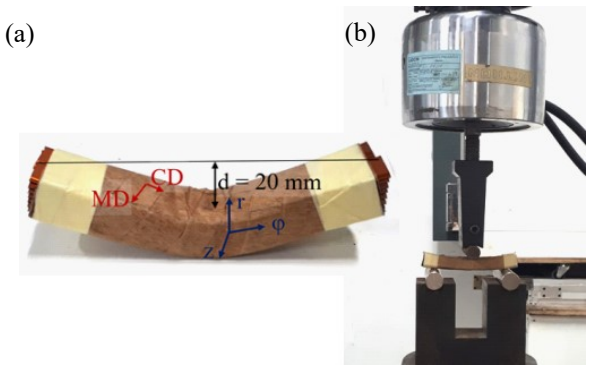

Figure 8. (a) CTC sample after the bending test with deflection d = 20mm, cylindrical coordinate system of a coil (r, φ, z) and main directions of the paper (MD and CD). (b) Three-point bending test of CTC samples.

2.3.2 Results of bending tests in paper-insulated CTCs

Several CTC samples of each of the ageing states (13 test conductor-pieces in total) were subjected to three-point bending tests under displacement control, Figure 8, up to different final deflections (d) which could be reasonably produced by severe short-circuit forces, according to experimental results of [1].

Figure 9 shows the results of each bending test, as well as their arithmetic average and the standard deviations, and there are considerable differences among the force–displacement curves. Firstly, the response of the non-aged samples considerably differs from that of the aged ones, because in the first, the copper strands are not glued by the enamel melting, and the relative sliding among them takes place since the beginning of the test. In the aged samples, the bonding between adjacent strands makes the assembly stiffer, but it gradually disappears as the deformation increases. Secondly, the position of the transposed strand varies in the different samples, so the way in which strands slide on each other also differs. Thus, the vertical force needed to produce a certain deflection is highly variable, and abrupt steps are produced when the bonding breaks.

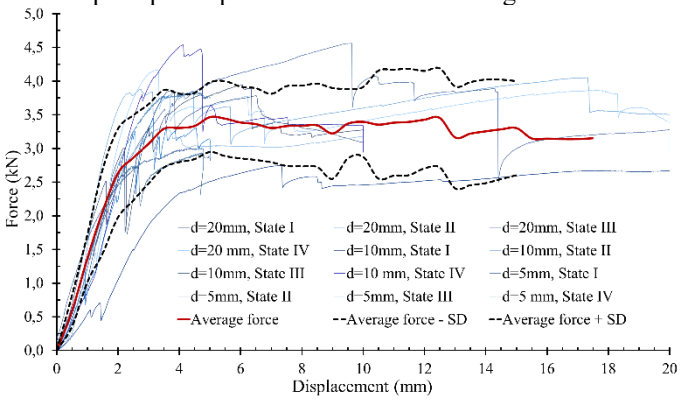

Figure 9. Results of bending tests on the aged CTC samples with different deflections (d) and ageing states.

2.4 FAILURE OF PAPER

2.3.3 Macroscopic analysis of fracture patterns

After the bending tests, the magnitude of the fractures in the layers of the insulation was measured and classified in Table 1

into: no cracks, small cracks (<5 mm), medium cracks (5-10 mm), big cracks (>10 mm), and total fracture (paper so deteriorated that it does not accomplish any insulating purpose).

Table 1. Fracture sizes in the paper as a result of bending tests in the CTC.

		DEFLECTION IN THE BENDING TEST		
	Layer	d = 20 mm	d = 10 mm	d = 5 mm
Ageing State 0	1 2 3 4	*No cracks*	*No cracks*	*No cracks*
Ageing State I	1 2 3 4	*Big cracks* *Medium cracks* *No cracks* *No cracks*	*Big cracks* *Small cracks* *No cracks* *No cracks*	*Small cracks* *No cracks* *No cracks* *No cracks*
Ageing State II	1 2 3 4	*Big cracks* *Big cracks* *No cracks* *No cracks*	*Big cracks* *Small cracks* *No cracks* *No cracks*	*Small cracks* *No cracks* *No cracks* *No cracks*
Ageing State III	1 2 3 4	*Total fracture* *Total fracture* *Small cracks* *Small cracks*	*Total fracture* *Big cracks* *No cracks* *No cracks*	*Medium cracks* *No cracks* *No cracks* *No cracks*
Ageing State IV	1 2 3 4	*Total fracture* *Total fracture* *Big cracks* *Big cracks*	*Total fracture* *Big cracks* *Medium cracks* *Medium cracks*	*Big cracks* *Big cracks* *Small cracks* *Small cracks*

In Ageing State 0, both the plain and the crepe papers were able to withstand d = 20 mm without fractures in any of the layers. The effect of the extreme thermal ageing in the oil-impregnated paper is of great relevance, especially in the plain Kraft, and after only a week of ageing (Ageing State I), fractures appeared systematically in layer 1 regardless of the final deflection of the CTC and in layer 2 for d > 10 mm.

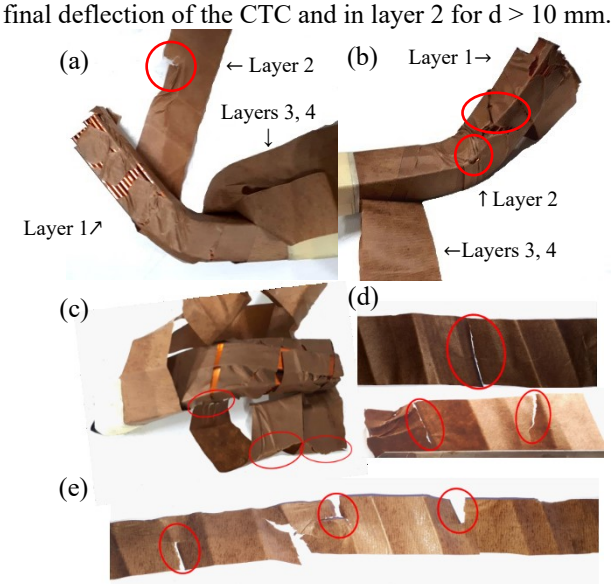

Figure 10. Results for d = 20 mm in (a) Ageing State I, (b) State II, (c) inner layers in State III and (d) layer 2 and (e) layer 4 in State IV.

The difference between Ageing States I and II was not very marked, except when d = 20 mm, where the cracks in the two inner layers were more accused, Figure 10a and Figure 10b. The effects of ageing markedly increased in State III, where d = 5 mm was enough to produce relevant cracks in layer 1, d = 10 mm produced big cracks in layers 1 and 2 , Figure 10c, and d = 20 mm started the fracture in the crepe paper. After 28 weeks, in Ageing State IV, both materials were in a very bad condition. Any d > 5 mm produced big fractures in the plain Kraft paper and small cracks in the crepe paper, which grow with the increase in the deflection, Figure 10d and Figure 10e.

In the CTC samples, the arrangement of the transposed strand, which is more affected by large deformations, is asymmetrical. Thus, some of the first cracks in the inner layer appeared near this strand, as seen in Figure 11. Besides, layer 1 was glued to the strands and broke on the sides of the CTC sample when sliding on each other. In the other layers, one common source of stress concentrations was the wrapping of the paper around the CTC, where most of the cracks were initiated, at an angle of approximately 70º from MD, because the pretension imposed on the paper during manufacturing made that direction weaker.

Figure 11. Transposed strand of the CTC and paper layer 1 in Ageing State IV and d = 5 mm.

2.3.4 Scanning Electron Microscope (SEM) analysis of fracture patterns

SEM is commonly used for the observation of specimen surfaces. The different microstructure of non-damaged plain Kraft and crepe papers can be seen in Figure 12. In Figure 12a, the matrix in which the cellulose fibres are embedded is less dense and the voids are more visible. In Figure 12b, the visible wrinkles are a characteristic of the manufactured material and their extension causes its hyperelasticity. The preferential orientation of the fibres in MD is more evident in crepe paper. Those microscopic structures are maintained in non-damaged areas of the insulation during the ageing process, indicating that crack initiation and growth is mostly a local phenomenon.

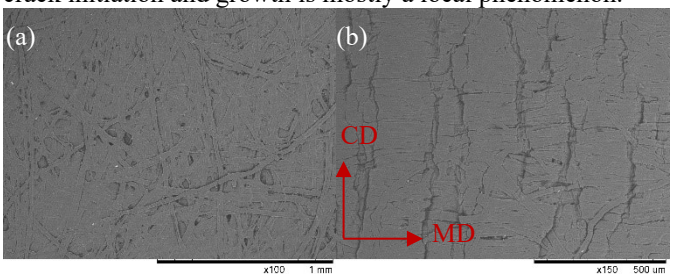

Figure 12. (a) Plain Kraft paper in layer 2 and (b) crepe paper in layer 3.

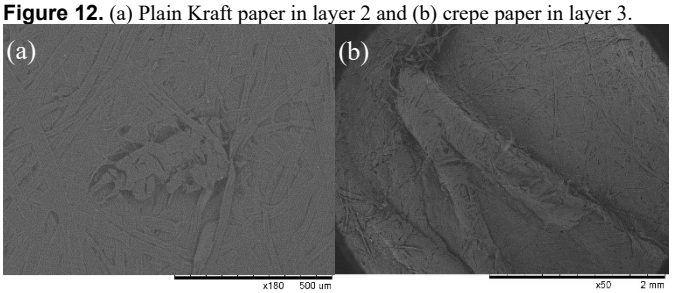

Figure 13. (a) Local defect and (b) wrinkle produced by the bending test, both in layer 2 and Ageing State II.

The purpose of using SEM here was to capture fracture initiation, and to better understand the fracture growth process that leads to big cracks or total failure of the material. Two types of defects were noticed: local defects initially present in areas of the material subjected to tension, Figure 13a, which suffered stress concentrations due to the large deformations of the CTC

and grew as a result; in areas subjected to compression, wrinkle formation can also result in cracks when the paper is heavily aged, Figure 13b. Other fractures in the material observed with SEM are shown in Figure 14.

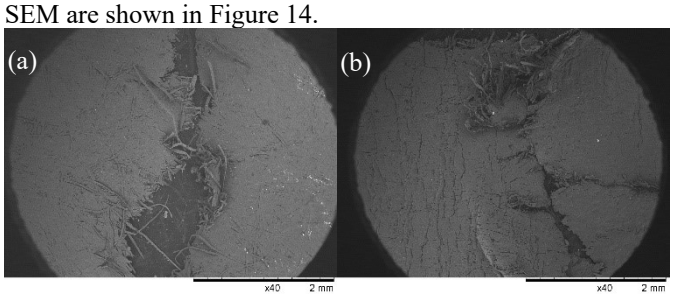

Figure 14. (a) Part of a medium-size crack in layer 2 and Ageing State I; (b) small crack in layer 4 and Ageing State III.

3 NUMERICAL SIMULATION

A finite element (FE) mechanical model was implemented in ANSYS AIM Static Structural, to reproduce the strains in the copper CTC sample that will subsequently affect the insulation.

3.1 GEOMETRY, SUPPORTS AND MATERIAL PROPERTIES

The CTC consists of two independent stacks, named as A and B, each of them formed by eight copper strands, plus the transposed one, Figure 15a. For the sake of simplicity, both the curvature and the transposition in the CTC were ignored in the model, as in [4]. Previously in [16], a solid rectangular cross-section was modelled, and the final deflection numerically obtained was significantly lower than the experimental one, which confirms the need for the inclusion of the individual strands and the sliding between them, Figure 15b. An approximate symmetrical cross section was modelled in SpaceClaim, composed of 18 rectangular strands (nine in each stack) of 11 x 1.9 mm with rounded corners, Figure 15c. The strands are flexible solids with a nonlinear mechanical behaviour and length of 120 mm, made of annealed copper used in power transformers (Young's Modulus: 110 GPa; Poisson's Ratio: 0.34; Tensile yield strength: 220 MPa). The diameters of the loading and supporting cylinders were 20 mm and 25 mm, respectively; they were defined as rigid elements since they are considerably stiffer than the copper CTC.

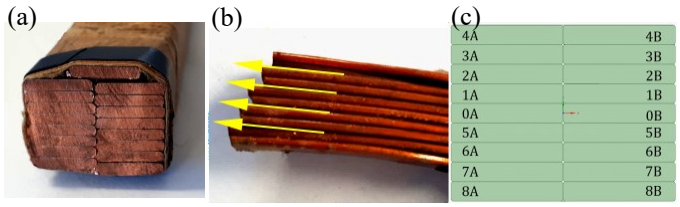

Figure 15. Cross-sectional view of the (a) real CTC, (b) initial sliding planes in the CTC sample after the bending test and (c) modelled CTC.

Two remote displacements impeding all degrees of freedom were applied to the bases of the support cylinders. In the base of the loading cylinder, a remote displacement was applied, impeding all the degrees of freedom except the *Y*-Component which was set as "*Free*", to transmit the bending load, Figure 16. As the bending test in the laboratory was carried out under displacement control, the displacement of the load cylinder was varied in the different steps during the simulation, and the force reaction in the contact with the CTC was measured, using *direct solver* type and *large deflections*.

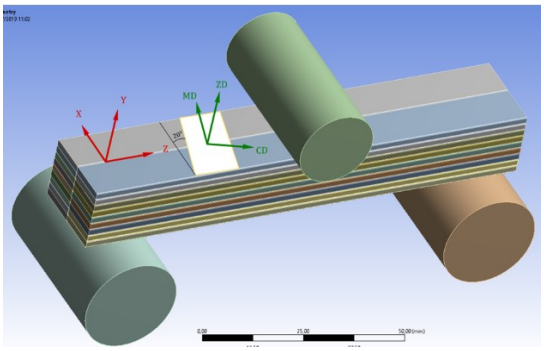

Figure 16. 3-D view of the CTC sample with the loading cylinder and the two supporting cylinders, with the coordinate systems of the CTC model (X, Y, Z) and of the paper material (MD, CD, ZD).

3.2 CONNECTIONS AND MESH DEFINITIONS

Defining the contact between the four layers of dielectric paper and their contact with the copper core is a numerical challenge, due to the small thickness of the layers of about 80 µm. Since one copper strand is almost 24 times thicker than one paper layer, the compatibility between adjacent meshes implies that the mesh size must be significantly smaller than the paper thickness; this entails an unmanageable number of elements for the whole model. Since the contribution of the insulation to the mechanical response of the CTC is negligible, the FE model did not include the paper. Due to the adherence between the insulation and the copper core, the strain field of the paper can be assimilated with the strain field at the surface of the CTC.

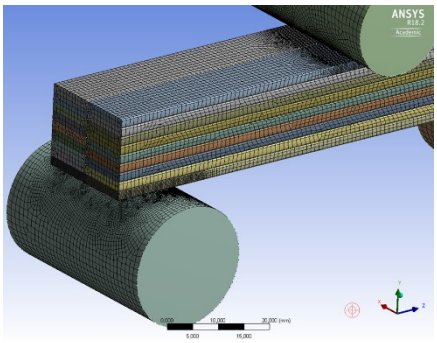

Figure 17. Close view of the mesh sizing of 0,25 mm in the contact between the cylinders and copper strands.

The definition of the mesh is crucial to guarantee the model reliability. A *mechanical-type mesh* with a relevance of 100 and *curvature* was chosen. *Fine* relevance centre and *slow* transition were selected for the size function, since more elements are needed in the rounded corners of the strands, to avoid sharp edges that could lead to stress concentrations. An overall minimum element size of 1 mm was used in the 18 strands. To avoid convergence problems in the contacts between the cylinders and the CTC, some *element size on contacts* of 0.25 mm were introduced in these regions, see Figure 17. The model consists of approximately 350,000 elements.

Different analyses with variable frictional coefficients were carried out in order to capture, firstly, the elastic part of the

force-deflection curve obtained in the laboratory, concluding that a *frictional contact* with a coefficient of 2 was the one that better captured the CTC behaviour under bending. The *Augmented Lagrange* formulation was used, with a normal stiffness factor of 0.01 updated in *Each Iteration*, because that permitted a less rigid contact and facilitated convergence under bending deformation [17]. In the contacts between the rigid cylinders and a strand, the normal stiffness was updated in *Each Iteration,* and the *Aggressive* option was selected.

After the initial elastic part of the curve, the sliding between adjacent strands affected the response more than the plastification of the copper. Sliding produced abrupt decreases in the force at some points in the force-displacement curve. That phenomenon was modelled with a reduction of the frictional coefficient from 2 up to 0.5 at some steps of the analysis, included by inserting some *commands* through APDL into the contacts between copper strands. It had been noticed in the laboratory that the initial planes of sliding appeared between pairs of strands, Figure 15c, and if the deformation continued, the bonding between individual strands also broke afterwards.

3.3 RESULTS

The results of the FE simulation and the experiments (arithmetic average of the results of all the tests and the standard deviation) show a notable agreement, Figure 18. The abrupt decreases in the force at some levels of deformation represent the initiation of the sliding between two adjacent strands.

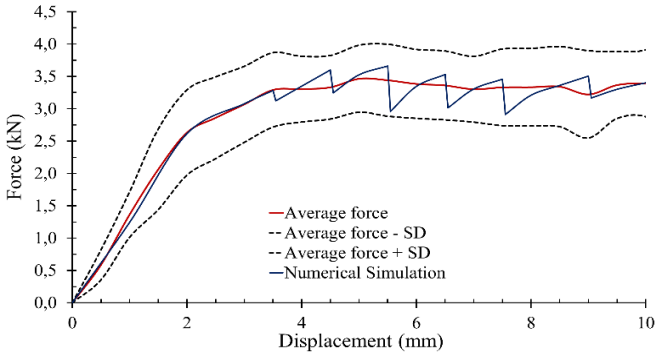

Figure 18. Comparison of the experimental and simulated force-displacement curve up to a final d = 10 mm.

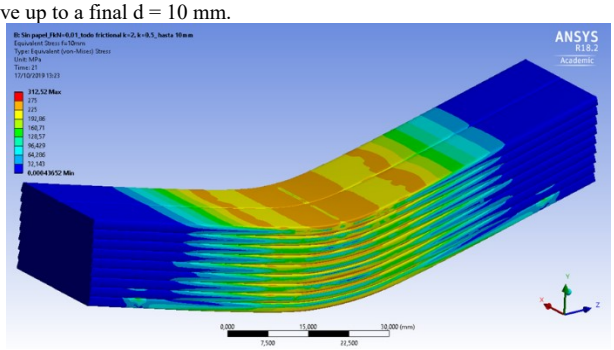

Figure 19. Equivalent (von-Mises) stress, in MPa, for the simulated bending test with final d = 10 mm.

The equivalent stress of the CTC is relevant because it determines which areas of the copper conductor will plasticise. In those areas, the deformation is non-reversible and larger than in the non-plasticised ones, so the deformation of the insulation will also be higher. The central area, in the contact with the load cylinder, is the most stressed, with stresses higher than 200 MPa, Figure 19, and will be the first to undergo irreversible deformations. The model shows a relevant growth in the extension of plasticised areas in the CTC sample when the final deflection rises from 5 mm to 10 mm.

The most relevant data for the construction of a failure model for the paper insulation is the strain field. In the numerical model, the strains can be obtained referred to the principal axes of the geometry (X, Y, Z), which do not coincide with the main directions of the paper material (MD, CD, ZD). In the upper and lower faces of the CTC, which are the most stressed ones, Y-direction coincides with ZD, and directions (MD, CD) can be obtained after performing a clockwise rotation of $\theta = 20^{\circ}$ in axes (X, Z), see Figure 16. If the strains in the original coordinate system are known, the strains in the coordinate system of the paper can be obtained from:

$$\varepsilon_{MD} = \varepsilon_X cos^2\theta + \varepsilon_Z sin^2\theta + \gamma_{XZ} \sin\theta \cos\theta$$

$$\varepsilon_{CD} = \varepsilon_X sin^2\theta + \varepsilon_Z cos^2\theta - \gamma_{XZ} \sin\theta \cos\theta$$

$$\gamma_{MD-CD} = 2(\varepsilon_Z - \varepsilon_X) \sin\theta \cos\theta + \gamma_{XZ}(cos^2\theta - sin^2\theta)$$

(a)

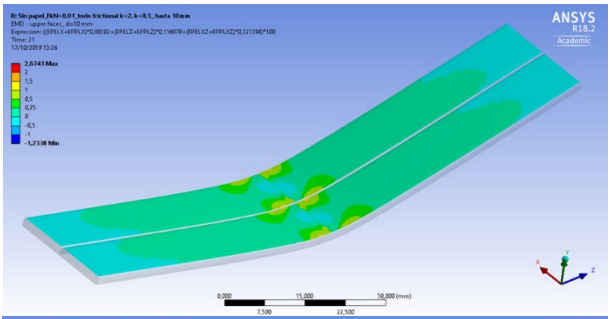

(b)

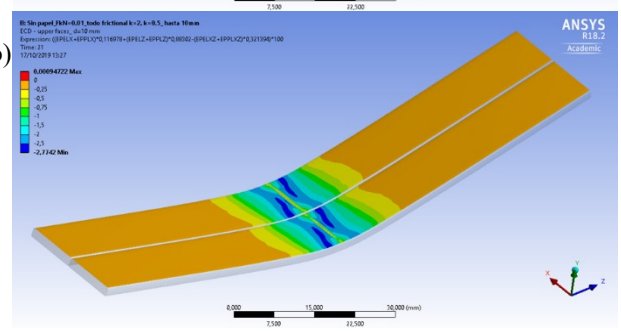

Figure 20. Strain (%) in (a) MD and (b) CD, in the upper face of the CTC with a final d = 10 mm.

Figure 20 and Figure 21 show the total strain in MD and CD when d = 10 mm. There are areas subjected to tension and others subjected to compression in both in the upper and lower faces of the CTC, but, as only the tensile mechanical properties of the insulation have been obtained here, only the failure in tension can be analysed. Almost the whole upper surface, Figure 20, is subjected to tension in MD (with maximum values in the centre between 0.5-2.67%), and to compression in CD (maximum values between 1-2.77%). With respect to the lower surface, Figure 21, it is mostly subjected to compression in MD (between 0.5-0.72%), and to tension in CD (between 1.5-2%).

It is coherent that no cracks appeared in the insulation in Ageing State 0, when d=10 mm, as both ε_{MD}^{max} and ε_{CD}^{max} for the plain Kraft and the crepe insulations were much higher than the maximum strains numerically obtained (see Figure 5b and Figure 7b). The appearance of cracks in State IV is also

coherent, as the simulation gives tensile strains higher than 2%, while the experiments over both types of insulation gave ε_{MD}^{max} between 0.68-2.30% and ε_{CD}^{max} between 1.45-1.75%. In the intermediate ageing states (I, II and III), the maximum strains at break of the crepe paper ($\varepsilon_{MD}^{max} > 17\%$ and $\varepsilon_{CD}^{max} > 3.44\%$) were still much higher than the values numerically obtained, so the model can justify that no cracks appeared. However, the failure of the plain Kraft insulation in states I, II and III cannot be explained by the maximum tensile strain criterion, because the experimental ε_{MD}^{max} was higher than the strains given by the simulation, and ε_{CD}^{max} was only exceeded in very small areas which were not compatible with the size of the produced cracks. In those states, the interaction of tension, compression and shear strains must have played a role in crack initiation and growth.

(a)

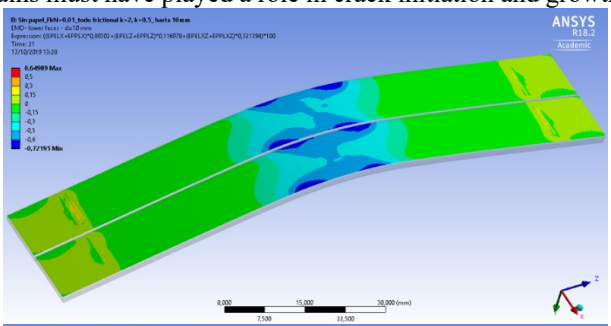

(b)

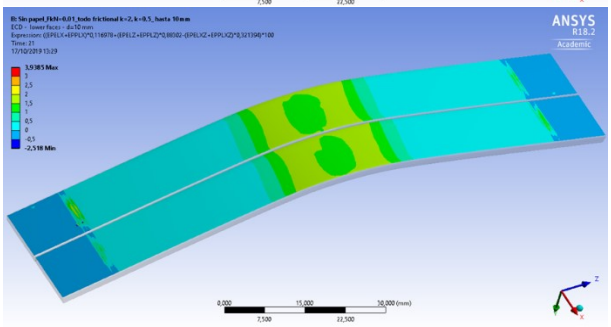

Figure 21. Strain (%) in (a) MD and (b) CD, in the lower face of the CTC with a final d = 10 mm.

4 CONCLUSIONS

The present analysis was aimed at characterising failure modes of the paper insulation in CTCs used in power transformers, and led to the following conclusions:

- Regarding the disposition of the different paper layers, failure will always start in the most inner one if the enamel melts. In that layer, crack-initiation starts near the transposed conductor, and in the sides of the CTC, where there is a sliding between copper strands. In layers 2, 3 and 4, the preferential direction for the cracks coincides with the edges in the wrapping of the insulation around the CTC.
- The initial properties of the crepe paper were much better than the ones of the plain Kraft paper but, they were more affected by the extreme thermal ageing.
- There were no significant differences in the impact of ageing between layers 3 and 4. Being in direct contact with the dielectric oil (as in the case of layer 4) was not relevant.
- When the paper is heavily aged and fragile, wrinkles in areas subjected to compression are more critical for crack initiation and growth than areas subjected to tension.
- The sliding between adjacent strands is an essential feature of the response of CTCs under bending. The presented mechanical FE model can represent the mechanical response of the copper CTC to a bending force quite accurately.

These experimental results and this simulation model are relevant for the characterisation of failure modes of the paper insulation in CTCs and can be used for the development of an analytical failure criterion, where compressive and shear strengths of the material should be also considered in order to obtain accurate predictions.

ACKNOWLEDGMENT

The authors gratefully acknowledge the contribution of Ivo Fernández for his help with the preparation of the test pieces, and David John Cahill for the revision of English language.

REFERENCES

[1] G. Bertagnolli, *Power Transformers and Short Circuits. Evaluation of the short-circuit performance of power transformers*, ABB. 2014.

[2] K. Karsai, D. Kerényi, and L. Kiss, *Large Power Transformers*. Budapest: Elsevier, 1987.

[3] D. Geissler and T. Leibfried, "Short circuit tests to derive the buckling strength of Continuously Transposed Cable for power transformers under the influence of the paper insulation thickness," *Power Engineering Conference (UPEC)*, 2014, vol. 32, no. 4.

[4] D. Geissler and T. Leibfried, "Mechanical breakdown of aged insulating paper around continuously transposed conductors for power transformers under the influence of short-circuit forces - Analysis by numerical simulations," *Electr. Insul. Conf.(EIC)*, 2015, pp. 401–406.

[5] D. Geissler and T. Leibfried, "Short-Circuit Strenght of Power Transformer Windings-Verification of Tests by a Finite Element Analysis-Based Model," IEEE Trans. Power Del., vol. 32, no. 4, pp. 1705–1712, 2017.

[6] Y. Li *et al*, "Insulation Performance of Aging Transformer Winding under Transient Impulse," *IEEE Int. Conf. Dielectr. Liquids (ICDL),* 2017, pp. 1–4.

[7] H. Ye *et al*, "Insulation Characteristics of Deformed Transformer Winding under Transient Impulse," *Annu. Rep. Conf. Electr. Insul. Dielectr. Phenom. (CEIDP)*, 2017, pp. 552–555.

[8] E. Borgqvist *et al*, "Dielectric properties of polymers," *Tappi*, vol. 19, no. 1, p. 634, 2014.

[9] O. Girlanda, K. Wei, T. Brattberg, and L. E. Schmidt, "Influence of Density on the Out-of-Plane Mechanical Properties of Pressboard," *Annu. Rep. Conf. Electr. Insul. Dielectr. Phenom. (CEIDP)*, 2012, pp. 247–250.

[10] O. Girlanda *et al*, "Analysis of the Micromechanical Deformation in Pressboard performed by X-ray Microtomography," *IEEE Electr. Insul. Conf.(EIC)*, pp. 89–92, 2015.

[11] T. Joffre *et al*, "A 3D in-situ investigation of the deformation in compressive loading in the thickness direction of cellulose fiber mats," Cellulose, vol. 22, no. 5, pp. 2993–3001, 2015.

[12] O. Girlanda *et al,* "Static and quasi-static behavior of dry and oil-impregnated pressboard," *IEEE Electr. Insul. Conf. (EIC)*, 2016, pp. 105–108.

[13] Insulating liquids - Oil-impregnated paper and pressboard - Determination of water by automatic coulometric Karl Fischer titration, IEC 60814, 1997.

[14] Measurement of the average viscometric degree of polymerization of new and aged cellulosic electrically insulating materials, "IEC 60450, 2007.

[15] Paper and board. Determination of tensile properties. Part 2: Constant rate of elongation method (20 mm/min), ISO 1924-2:2008, 2008.

[16] C. Oria *et al,* "Mechanical Behaviour of the Cellulosic Dielectric Materials of Windings in Power Transformers in Operation," *IEEE Int. Conf. Electr. Machines, (ICEM)*, 2018, pp. 2400–2406.

[17] R. Afshar *et al,* "Comparison of experimental testing and finite element modelling of a replica of a section of the Vasa warship to identify the behaviour of structural joints," Eng. Struct., vol. 147, pp. 62–76, 2017.